NANO · MICRO small
www.small-journal.com

Check for updates

Piezocatalysis for Chemical–Mechanical Polishing of SiC: Dual Roles of t-$BaTiO_3$ as a Piezocatalyst and an Abrasive

Tao Hu, Jinxi Feng, Wen Yan, Shuanghong Tian,* Jingxiang Sun, Xiaosheng Liu, Di Wei, Ziming Wang, Yang Yu, Jason Chun-Ho Lam, Shaorong Liu, Zhong Lin Wang, and Ya Xiong*

Chemical mechanical polishing (CMP) offers a promising pathway to smooth third-generation semiconductors. However, it is still a challenge to reduce the use of additional oxidants or/and energy in current CMP processes. Here, a new and green atomically smoothing method: Piezocatalytic-CMP (Piezo-CMP) is reported. Investigation shows that the Piezo-CMP based on tetragonal $BaTiO_3$ (*t*-BT) can polish the rough surface of a reaction sintering SiC (RS-SiC) to the ultra-smooth surface with an average surface roughness (Ra) of 0.45 nm and the rough surface of a single-crystal 4H-SiC to the atomic planarization Si and C surfaces with Ra of 0.120 and 0.157 nm, respectively. In these processes, *t*-BT plays a dual role of piezocatalyst and abrasive. That is, it piezo-catalytically generates in-situ active oxygen species to selectively oxidize protruding sites of SiC surface, yielding soft SiO_2, and subsequently, it acts as a usual abrasive to mechanically remove these SiO_2. This mechanism is further confirmed by density functional theory (DFT) calculation and molecular simulation. In this process, piezocatalytic oxidation is driven only by the original pressure and friction force of a conventional polishing process, thus, the piezo-CMP process do not require any additional oxidant and energy, being a green and effective polishing method.

1. Introduction

With the growing requirements for high-power, high-temperature, and high-frequency optoelectronic devices, third-generation semiconductors have attracted a rising interest over the past decades.[1] Specially, since Tesla adopted SiC chips on electric vehicle Model 3 in 2018, the demand for SiC as power semiconductors has experienced an unprecedented surge.[2] For example, SiC-based UPS developed by Toshiba has reached 98.2%, and Toyota has replaced Si-based PIN diodes with 4H-SiC-based Schottky-barrier diodes in the DC converters of hybrid electric vehicles.[3] These semiconductors, specially epitaxial substrates for optoelectronic devices, are all required to possess ultra-precision, even atomically smoothing surfaces, in addition to the requirement for their excellent thermal stability and minimizing power loss, as the surface quality significantly impacts the performance of these semiconductors and final devices.[4] For instance, any micro-defect and scratch on the substrate surface will decrease the breakdown electric field intensity and charge.[5] Thus, the ultra-precision polishing has become one of most demanded research topics in the field of advanced materials.[3,6]

In the third-generation semiconductors, SiC is a dominant candidate with more excellent characteristics, compared with several state-of-the-art Si materials, such as its wide bandgap (2.3–3.2 eV), high break down field and high thermal conductivity (4.9 W m^{-1} K^{-1}) and thermal stability (3.8×10^{-6} °C^{-1}), high breakdown voltage (1×10^6–5×10^6 V·cm^{-1}) and low coefficient of thermal expansion (~1.4×10^{-6} K^{-1}).[3,7] However, its inherent high hardness (Moh's hardness 9.2) and chemical inertness bring many challenges to traditional polishing techniques.[8] For example, the mechanical polishing method can introduce scratches and subsurface damage to surface of SiC. Thus, in the 1980s, IBM first introduced the chemical mechanical polishing (CMP) technology and it has been extensively utilized to generate ultra-smooth and low-damage surfaces of semiconductor wafers presently.[5] However, these CMP processes consume a lot of additional energy and chemical reagents, such as H_2O_2,

T. Hu, J. Feng, W. Yan, S. Tian, J. Sun, X. Liu, Y. Xiong
School of Environmental Science and Engineering
Sun Yat-sen University
132 East Waihuan Road, Guangzhou 510006, P. R. China
E-mail: jinxfeng@cityu.edu.hk; tshuangh@mail.sysu.edu.cn
D. Wei, Z. Wang, Y. Yu, Z. L. Wang
CAS Center for Excellence in Nanoscience
Beijing Institute of Nanoenergy and Nanosystems
Chinese Academy of Sciences
Beijing 100083, P. R. China
J. Feng, J. C.-H. Lam
School of Energy and Environment
City University of Hong Kong
Kowloon Tong, Hong Kong SAR P. R. China
S. Liu
Department of Chemistry and Biochemistry
University of Oklahoma
Norman, OK 73019, USA

The ORCID identification number(s) for the author(s) of this article can be found under https://doi.org/10.1002/smll.202310117

DOI: 10.1002/smll.202310117

© 2023 Wiley-VCH GmbH

$FeCl_3$, $KMnO_4$, CrO_3, NaOH, HF, and ammonium cerium nitrate (IV), and simultaneously generate a lot of waste.[9] Furthermore, the frequently used HF is extremely corrosive and it can cause incurable burns if inhaled into the respiratory tract or contact with skin. Therefore, it is strongly desired to find new efficient and green polishing technology for developing electronic devices-based SiC.[9b]

Piezoelectric effect is a physical phenomenon of electromechanical conversion mediated by deformed piezoelectric materials. Although it was discovered 100 years ago by the Curie brothers, Pierre and Jacques, and has been widely applied to sensors, actuators, and high voltage generators, the piezoelectric effect of nano-materials was not observed until 2003.[10] Since then, the research on piezoelectric effect has entered a new flourishing period and its various uses have been constantly developed.[11] Among them, the piezocatalysis is one of the most interesting applications.[12] Recently, an increasing number of investigations about the piezocatalytic applications have been reported, such as piezocatalytic tooth whitening,[13] piezocatalytic sterilization,[14] piezocatalytic dechlorination,[12c] piezocatalytic advanced dewatering,[15] piezocatalytic tumor therapy[16] and so on. However, the piezocatalysis has still not been applied to the polishing field so far.

As we know, the piezocatalysis is a kind of special advanced oxidation technology driven by mechanical energy to generate high active oxygen species (•OH, $•O_2^-$ and H_2O_2 etc.). In the piezocatalysis, the used mechanical forces basically originated from ultrasonic wave, but recently a few researchers found that usual mechanical energies could also drive the piezocatalytic processes, such as agitation[17] and filtration pressure.[15] Therefore, according to the general principle of piezocatalysis and CMP,[18] it was expected that the piezocatalytic effect of nano piezo-materials as a polishing medium was driven by the pressure and friction between the polishing pad and workpiece and generated in-situ these highly active oxygen species to oxidize the SiC into SiO_2 and CO_2. Moreover, according to the principles of general tribology and the dependence of piezoelectric effect on pressure, it can be believed that the protrusions of SiC surface will be subjected to greater stresses than other positions, resulting in stronger piezocatalytic effect on these protrusions. Thus, it is expected that these protuberances will be preferentially oxidized, leading to the formation of a local soft SiO_2 layer. This process is different from the non-selective oxidation of electrochemical oxidation polishing.[9b] Then, this local new-formed soft SiO_2 layer was removed by mechanical abrasion of nano piezo-materials, resulting in a flattened SiC surface. In the process, the nano piezo material acted both as a piezocatalysis and an abrasive to selectively polish the soft oxide layer. The polishing process does not need any additional oxidants in usual CMP, and additional energy, such as photo-energy in photocatalytic CMP, electro-energy in electrocatalytic CMP, ultrasonic CMP (no piezocatalyst), and plasma polishing CMP. It can be considered a new kind of effective and "green" CMP technology. Its "green" characteristics attracted us to start a project for probing the new CMP process to create ultra and even atomically smooth surface of SiC. For the convenience of discussion, this CMP process was referred to as piezocatalytic CMP, abbreviated as "piezo-CMP".

Here, we report the proof-of-conception and application case of the new piezo-CMP process. In the process, tetragonal barium titanate (*t*-$BaTiO_3$, abbreviated as *t*-BT) was selected as both a piezocatalyst and an abrasive, and reaction-sinetred silicon carbide (RS-SiC) and single-crystal 4H silicon carbide (4H-SiC) are used as target workpieces because RS-SiC is a low an ideal mirror material of space telescope systems with a low manufacturing cost, and 4H-SiC is one of the most attractive semiconductor materials for the next-generation power device applications.[19] The aim of this investigation was mainly to approach two scientific issues: first, could the conventional polishing process drive efficiently the piezocatalytic effect and selectively oxidize much inert SiC to SiO_2 and CO_2? And second, could nano-piezomaterial perform the dual functions of a piezocatalyst and an abrasive, in addition to developing a green and efficient CMP process?

2. Results and Discussion

Generally, ultrasound is used as the driver of piezocatalytic process while using a polishing device as the driver of piezocatalytic process has not still been reported yet. Accordingly, a simulated polishing process using the degradation of a typical pollutant, methylene blue (MB), as an indicator was first tested whether the usual polishing device could drive the piezocatalytic process. As shown in **Figure 1**a,b, MB was apparently decolorized and degraded in the polishing process using both *t*-BT and *c*-BT (cubic $BaTiO_3$) as the abrasives without any additional chemicals in 20 min, but MB degradation efficiency in the former process was 15.4% higher than that in the latter process. As we know, *t*-BT was a kind of typical piezo-material while *c*-BT with a symmetrical center has no piezo-activity, although they are both barium titanate.[20] These functions were confirmed by Figure 1c, in which, except for adsorption, no MB degradation was observed, in an ultrasound-driven process using *c*-BT as the catalyst, while MB degradation reached 65.0% in the ultrasound-driven process using *t*-BT as the catalyst. Therefore, the difference of MB degradation from *t*-BT and *c*-BT abrasives could be attributed to the piezoelectric effect of *t*-BT driven by the polishing driver. In other words, the piezocatalytic oxidation process could be driven by the pressure and friction force from the usual polishing device and could obviously enhance the degradation of pollutants. While the degradation of MB for *c*-BT without no piezo-activity as abrasive could be attributed to the tribo-chemical effect in many mechanical processes, as reported by Mahrova et al.[21] As a result, MB degradation in the simulated polishing process using *t*-BT with piezo-activity as an abrasive could also not exclude the tribochemical contribution. However, it was affirmed that the piezocatalytic process driven by the usual polishing device could enhance the polishing efficiency of SiC, according to the great difference of MB degradation between *t*-BT and *c*-BT abrasives.

The efficient piezocatalytic degradation of the pollutant MB driven by the polishing device further encouraged us to experimentally investigate the feasibility of piezo-CMP principle for SiC because they were both involved in the piezocatalytic oxidation process. **Figure 2** shows the surfaces of RS-SiC before and after polishing. It could be seen from Figure 2a that the original RS-SiC showed a gray coarse surface. After polishing with *t*-BT the partial surface became a smooth black mirror-like (ca. 12 cm^2) that could clearly reflect objects, such as fingers (Figure 2b), while the surface of RS-SiC was only slightly flattered with *c*-BT as the polishing abrasive and could only vaguely reflect the

16136829, 2024, 21, Downloaded from https://onlinelibrary.wiley.com/doi/10.1002/smll.202310117 by Cas-Beijing Institution Of, Wiley Online Library on [28/05/2025]. See the Terms and Conditions (https://onlinelibrary.wiley.com/terms-and-conditions) on Wiley Online Library for rules of use; OA articles are governed by the applicable Creative Commons License

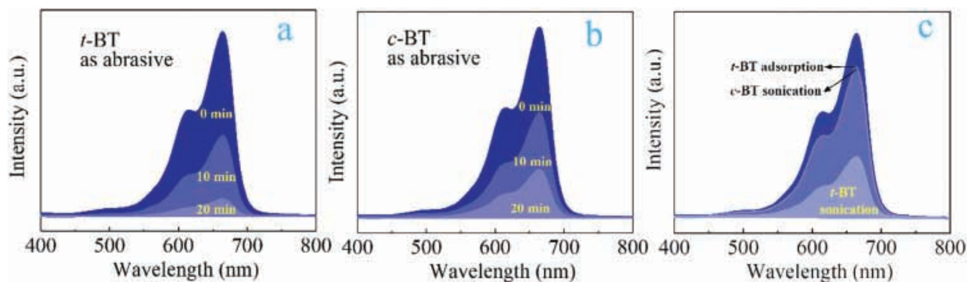

Figure 1. a) polishing using *t*-BT as abrasives; b) polishing using *c*-BT as abrasives; c) sonication using *c*-BT and *t*-BT as catalysts, respectively.

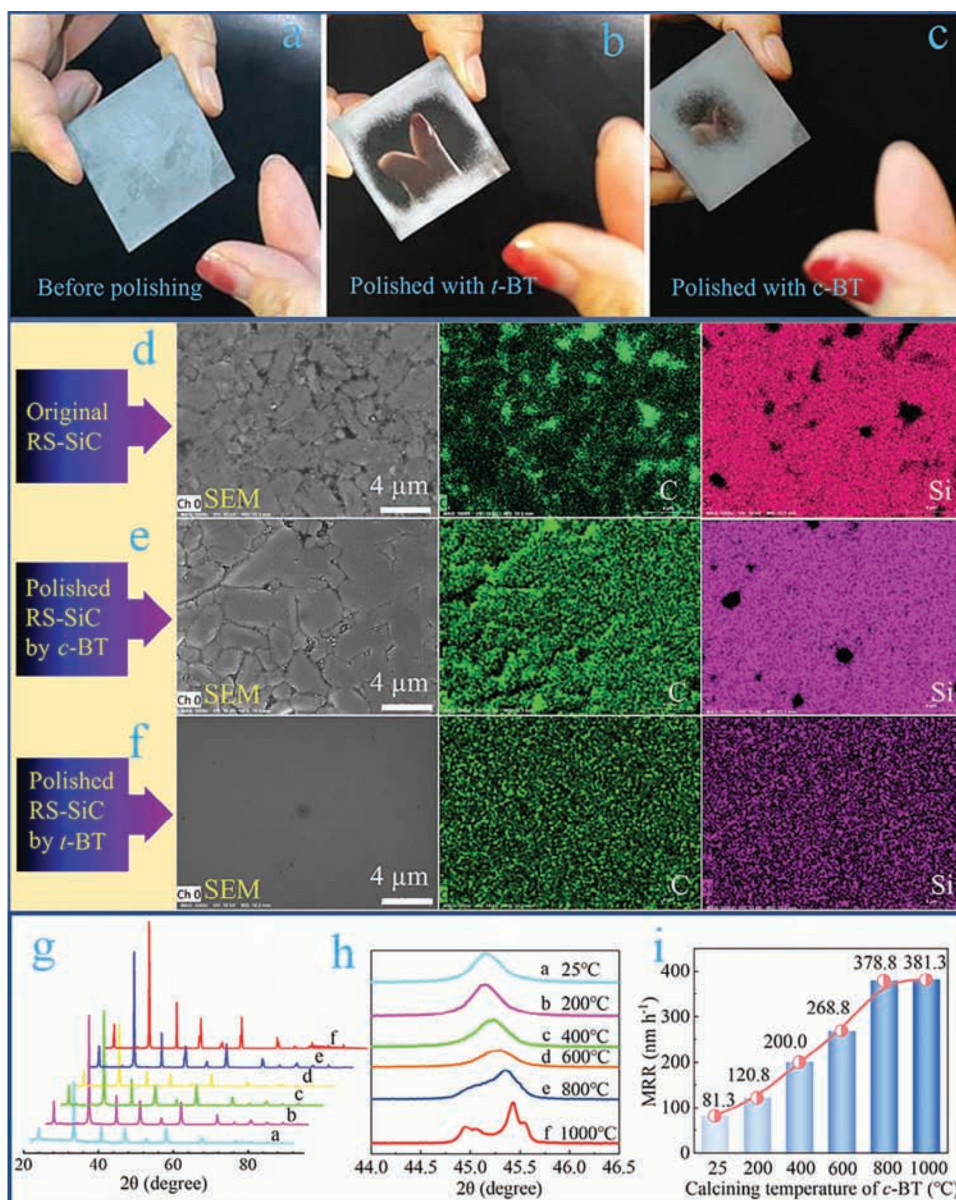

Figure 2. Experimental evidence of piezo-CMP as a new and green polishing technique. a, b, and c) Photo pictures of original and polished RS-SiC. d– f) SEM and elemental mappings of original and polished RS-SiC surface. g,h) Effect of calcination temperatures on XRD pattern. i) MRR of BT.

 © 2023 Wiley-VCH GmbH

16136829, 2024, 21, Downloaded from https://onlinelibrary.wiley.com/doi/10.1002/smll.202310117 by Cas-Beijing Institution Of, Wiley Online Library on [28/05/2025]. See the Terms and Conditions (https://onlinelibrary.wiley.com/terms-and-conditions) on Wiley Online Library for rules of use; OA articles are governed by the applicable Creative Commons License

16136829, 2024, 21, Downloaded from https://onlinelibrary.wiley.com/doi/10.1002/smll.202310117 by Cas-Beijing Institution Of, Wiley Online Library on [28/05/2025]. See the Terms and Conditions (https://onlinelibrary.wiley.com/terms-and-conditions) on Wiley Online Library for rules of use; OA articles are governed by the applicable Creative Commons License

fingers, as shown in Figure 2c. Scanning electron microscopy (SEM) and element mappings in Figure 2 could further show the differences of RS-SiC surface before and after polishing using *t*-BT and *c*-BT as an abrasive, respectively. For the original RS-SiC (Figure 2d), many stuck grains with various sizes and defects or potholes could be obviously observed from the SEM image, and its Si and C elements were non-uniformly distributed on its surface. Subjecting to polishing with *t*-BT (Figure 2e), RS-SiC presented a much flatter SEM surface without any apparent damage or scratches and Si and C were well-distributed. But polished with *c*-BT (Figure 2f), RS-SiC still remained a heterogeneous surface both in its SEM and elemental mappings.

As stated above, *t*-BT and *c*-BT were both $BaTiO_3$, but the former is a typical green piezoelectric material and the latter has no piezo-activity. Thus, it was concluded that the difference of these polishing processes originated from the discrepancy of their piezoelectric activity. In other words, the polishing process of RS-SiC with *t*-BT as the abrasive was significantly dependent on the piezocatalytic oxidation effect of *t*-BT.

It is well known that the content of *t*-BT increased with thermal treatment temperature of *c*-BT.[20] In order to confirm quantitatively the role of piezoelectric catalytic effect in the polishing, the material removal rate (MRR) of RS-SiC corresponding to the calcined *c*-BT at various temperatures was determined because the MRR was one of important indicators to confirm the effectiveness of a polishing technique.[22] As shown in X-ray diffraction spectra (XRD) (Figure 2g,h), barium titanate at 25 °C existed substantially in the crystal phase of *c*-BT, and with rising of its calcination temperature from 25 to 800 °C, and the content of *t*-BT was increased from 0.1% to 85.3%, which was obtained by the reported XRD calculation method.[23] Simultaneously, MRR of SiC increased from 80.3 to 378.8 nm h^{-1} and the MRR for 800 °C was 4.7 folds for 25 °C, as indicated in Figure 2i. The increase of MRR was consistent with that of *t*-BT crystal phase with piezo-activity, so that the enhanced effect of MRR with thermal treatment temperature could be attributed to its conversion of *c*-BT into piezo-active *t*-BT. The experimental results indicated further that the polishing process of RS-SiC was significantly dependent on the piezocatalytic effect of *t*-BT, while the slight polishing effect originated from the simple tribo-chemical oxidation (reaction (1))[24] and usual mechanical abrasion, like CeO_2 as abrasive. Therefore, it could be concluded that the polishing process of *t*-BT as abrasive was a kind of piezo-CMP process, as predicted above.

$$SiC + 2O_2 = SiO_2 + CO_2 \quad (1)$$

Based on the proof-of-concept of piezo-CMP, the dependence of the polishing effect of *t*-BT toward SiC on operation parameters was further quantitatively investigated. As shown in **Figure 3**a, the concentration of *t*-BT has a significant impact on the MRR. When *t*-BT increased from 0.0 to 80.0 mg mL^{-1}, MRR of RS-SiC was accelerated from 20.8 to 641.7 nm h^{-1}, increasing 30.9 times. For general mechanical polishing, the enhancement effect could be attributed to the increase of mechanic fraction sites with the increase of abrasive concentrations.[22] However, for the piezo-CMP, in addition to the fraction sites, more important origin of this enhancement effect was possible the increase of piezocatalytic active sites with the increase of *t*-BT, according to the principle of piezoelectric effect. It was also noticed that the max dosage was much less than that of reported abrasives in many polishing processes (Table S1, Supporting Information). For example, the Fenton-CMP reported by Zhang et al needs 20 wt% silica abrasives, in addition to 10 wt% $KMnO_4$ or 10 wt% H_2O_2 + 0.02 wt% Fe^{2+}.[25] From the perspective of abrasive usage, the piezo-CMP was also considered as a kind of greener polishing technology.

Figure 3b presents the dependence of MRR on the rotation speed of the polishing pad. It could be seen from the figure that the MRR increased nonlinearly from 40 to 512.5 nm h^{-1} with the increment of V from 20 to 100 r min^{-1}. Preston's equation was frequently used to explain the changes of MRR with the rotation speed in CMP technology. According to Preston equation[6]

$$MRR = kp\upsilon \quad (2)$$

where MRR is the material removal rate, k is the Preston coefficient, p is the applied pressure on the wafer surface, and υ is the relative velocity between the wafer and the polishing pad. MRR was a linear relationship between MRR and υ. The above experimental result of the piezo-CMP was inconsistent with Preston's equation. The difference was possible dependent on piezoelectric effect in piezo-CMP, because the Preston equation was only a classic equation to describe contact mechanics, and did not consider the effect of the piezo-catalysis.[6] For example, according to the following formulae of piezopotential:

$$V_p = \frac{\tau_y d_{xy} W_x}{\varepsilon_{rx}\varepsilon_0} \quad (3)$$

where, V_p is the piezo-potential, τ_y is the applied stress in the y direction, d_{xy} is the piezoelectric coefficient, W_x is the length of the all add-upped cell unit in the x direction, ϵ_{rx} is the relative permittivity in x direction, and ϵ_0 represented the permittivity of free space,[26] the piezoelectric potential was direct to the applied mechanical stress τ_y. Consequently, it could be inferred that the increase of the piezocatalytic effect with the rotational speed should be significantly responsible for the nonlinear increase in the piezo-CMP. Because piezo-CMP process was more complex than usual CMP processes, it has been difficult to explain their mechanism by only the simple Preston's equation.

Figure 3c presents the MRR of RS-SiC in *t*-BT slurry with various pH values. It could be seen that MRR was decreased by 26.3% at pH 3–7, however, considerably increased by 58.4% at pH 7–11. The facts were consistent with the observations in the usual CMP reported by Pan[22] and Yao et al.[24] The apparent increase of MRR could be ascribed to two reasons: Firstly, at high pH value, RS-SiC transferred favorably into easily removable SiO_2 and soluble silicate by the following friction chemical reactions (reaction (4) – (6)), as common CMP processes.[24]

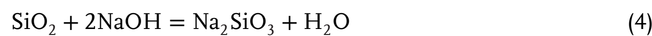

$$SiO_2 + 2NaOH = Na_2SiO_3 + H_2O \quad (4)$$

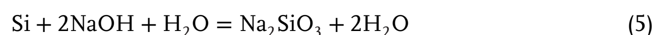

$$Si + 2NaOH + H_2O = Na_2SiO_3 + 2H_2O \quad (5)$$

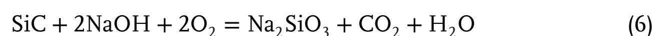

$$SiC + 2NaOH + 2O_2 = Na_2SiO_3 + CO_2 + H_2O \quad (6)$$

Here, Si represented the Si bond of SiC. Second, as we know, the occurrence of OH^- was beneficial to the generation of strongly oxidative •OH in the piezocatalytic processes.[12c,27]

 © 2023 Wiley-VCH GmbH

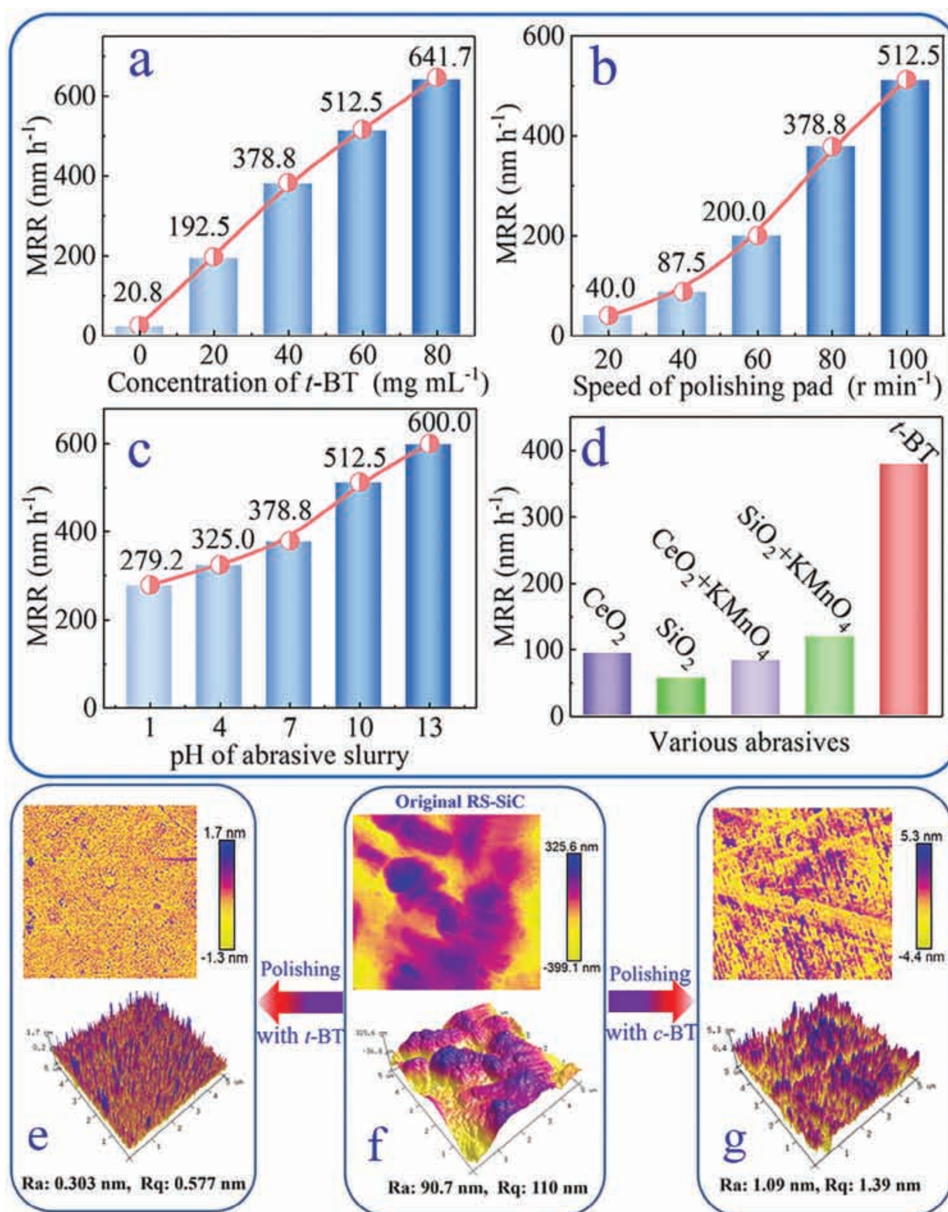

Figure 3. Effectiveness of *t*-BT Piezo-CMP toward RS-SiC. Up section: Effect of polishing conditions on the effectiveness (a: concentrations of *t*-BT, b: speed of polishing pad, c: pH, d: type of abrasive). Below section: AFM images of original and polished RS-SiC (e: polished with *t*-BT. f: original *t*-BT. g: polished with c-BT. Ra: average surface roughness, Rq: root mean square roughness.

Therefore, the increase of MRR was also possibly dependent on the generation of more •OH in *t*-BT slurry with high pH.

Figure 3d presented MRR values of RS-SiC in various CMP processes. It could be seen that for RS-SiC, the MRR of piezo-CMP increased much more rapidly than those of conventional CMP possesses. For example, the former was 4.0, and 6.7 folds of CMP possessed with CeO_2 and SiO_2, respectively. Even if strong oxidant $KMnO_4$ was added to enhance the polishing of CeO_2 and SiO_2, the MRR of piezo-CMP was still more than their MRR by 3.2 and 4.5 folds. The comparable tests indicated clearly that piezo-CMP was a kind of green and cost-effective precision polishing technology.

Considering that the average surface roughness (Ra) was another important indicator to evaluate the polishing performance, which was related to the polishing quality of workpieces, the changes of Ra were determined by atomic force microscopy (AFM). As displayed in Figure 3f, the original RS-SiC presented a coarse appearance with a Ra of 90.7 nm. After being subjected to *t*-BT polishing (Figure 3e), RS-SiC showed an ultra-smooth surface with a Ra of 0.30 nm and virtually without any scratch, while *c*-BT as abrasive only reduced its Ra to 1.09 nm and resulted in many scratches with a maximum surface depth of 9.7 nm (Figure 3g). This further indicated that the piezo-CMP of *t*-BT was more effective than that of the mechanical polishing of

© 2023 Wiley-VCH GmbH

16136829, 2024, 21, Downloaded from https://onlinelibrary.wiley.com/doi/10.1002/smll.202310117 by Cas-Beijing Institution Of, Wiley Online Library on [28/05/2025]. See the Terms and Conditions (https://onlinelibrary.wiley.com/terms-and-conditions) on Wiley Online Library for rules of use; OA articles are governed by the applicable Creative Commons License

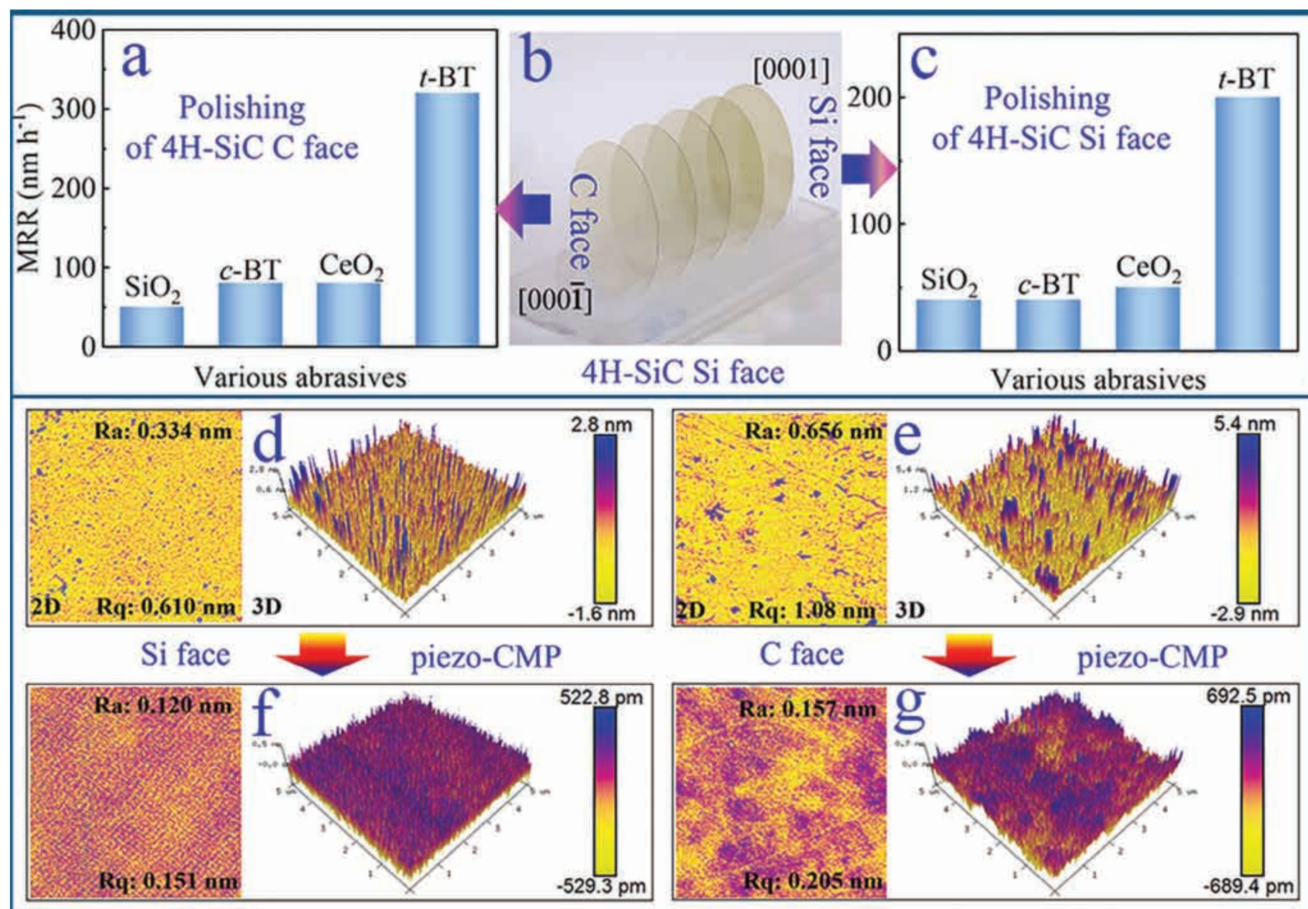

Figure 4. Effectiveness of *t*-BT piezo-CMP toward various crystal faces of 4H-SiC. Up part: Effect of abrasive type on the effectiveness (a: for C face of 4H-SiC, b: photopicture of 4H-SiC crystal, c: for Si face of 4H-SiC). Below part: AFM images of various crystal faces of original and polished 4H-SiC (d: original Si face. e: original C face. f: polished Si face. g: polished C face).

c-BT. To our knowledge, many groups researched the smoothing of RS-SiC, but few of them could yield an ultra-smooth surface. In fact, it was much more difficult to polish RS-SiC to a Ra value lower than 0.5 nm by CMP because the composition and structure of RS-SiC are not uniform.[28] For example, Shen et al. used anodic oxidation to polish RS-SiC to an Ra surface roughness of 2.103 nm while 4H-SiC to an Ra surface roughness of 0.892 nm.[19] Although Shen et al. could polish RS-SiC to an Ra surface roughness of 0.480 nm, it needs a two-step polishing process, that is, a 90-min water vapor plasma oxidation (0.864 nm) followed by a 40-min ceria slurry polishing.[29] Herein, the piezo-CMP offers a convenient protocol to reach below 0.5 nm in one-step. Moreover, it was especially worth mentioning that, in the process of this piezo-MCP, no additional oxidant and/or energy was added, except the electric power of the usual polishing device. These facts and analysis indicated that the piezo-MCP was a kind of potential green and deep polishing technique for RS-SiC.

In the SiC family, although RS-SiC has the unique advantage of low manufacturing cost, which makes it an ideal mirror material for space telescope systems, single-crystal SiC, such as 4H-SiC, has attracted more attention for its extraordinary capabilities as a representative of third-generation semiconductors working under high voltage and high frequency.[18b,30] However, it has an extremely high hardness (next only to the hardest diamond) and strong chemical stability, which needs an improved technique to polish its surfaces to meet the flatness requirement of third-generation semiconductors (generally >0.3 nm for Si-face and 0.5 nm for C-face), therefore, piezo-CMP was also tested to polish the super hard 4H-SiC. As shown in **Figure 4**, 4H-SiC was a light-yellow transparent crystal (Figure 4b), and its polishing rate and surface quality varied significantly with crystal orientations and abrasives. MRR of *t*-BT could also reach 318.8 nm h^{-1} for C face and 191.7 nm h^{-1} for Si face, respectively (Figure 4a). They were 3.3 times for C face and 3.6 times for Si face than that of *c*-BT, respectively (Figure 4c). This superiority of *t*-BT over *c*-BT could confirm again the great role of piezo-catalytic effect in the polishing of SiC, as aforementioned. In addition, it could still be seen from the figure that *t*-BT possessed a much faster polishing speed than the usual abrasives SiO_2 and CeO_2, although their Moh's hardness was greater than that of *t*-BT (SiO_2: ≈7.0, CeO_2: ≈6.0 and BT: ≈5.0). For the C face, the MRR of *t*-BT was 3.8 and 3.2 times higher than those of SiO_2 and CeO_2 individually, and while these numbers changed to 5.5 and 3.0 for the Si face. The MRR of *t*-BT was also much higher than those of the reported CMP processes recently reviewed by Hsieh et al.[18b] For example, the MRR of electrochemical-CMP reported by Murata et al

 © 2023 Wiley-VCH GmbH

16136829, 2024, 21, Downloaded from https://onlinelibrary.wiley.com/doi/10.1002/smll.202310117 by Cas-Beijing Institution Of, Wiley Online Library on [28/05/2025]. See the Terms and Conditions (https://onlinelibrary.wiley.com/terms-and-conditions) on Wiley Online Library for rules of use; OA articles are governed by the applicable Creative Commons License

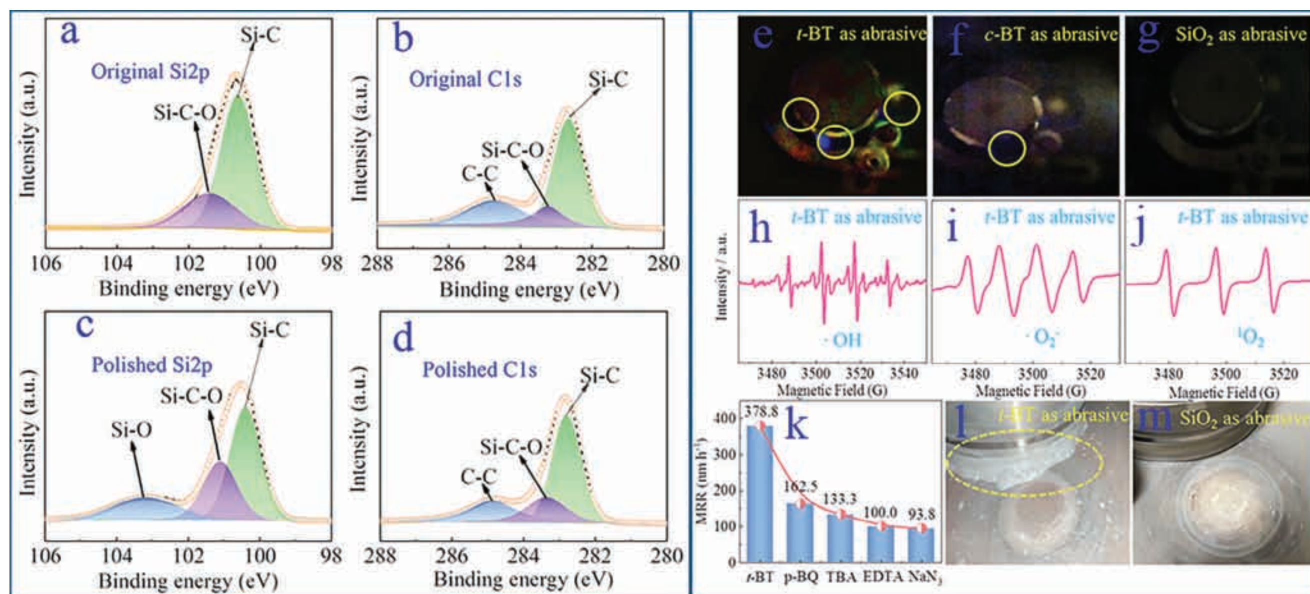

Figure 5. Evidence of piezocatalytic oxidation in the polishing process. Left: XPS spectra of original and polished RS-SiC (a: Si 2P of original RS-SiC, b: C1s of original RS-SiC, c: Si 2P of polished RS-SiC, d: C1s of polished RS-SiC). Right: radicals from piezo-CMP process (e, f, and g: chemiluminescence of oxidative radicals from polishing processes with various abrasives, h, i and j: ESRs of •OH, $•O_2^-$ and $^1O_2$, respectively, k: scavenging tests of radicals, l: generation of bubbles, m: no bubble).

only reached the range of 115–950 nm h^{-1}.[30] These facts indicated that *t*-BT as both abrasive and piezocatalyst was also more efficient, and it holds a great potential to replace the usual abrasives especially for super hard 4H-SiC.

Figure 4 also presented AFM of 4H-SiC before and after polishing with *t*-BT. The original 4H-SiC presented forest-like Si and C faces with Ra of 0.334 and 0.656 nm, respectively (Figure 4d,e). After piezo-CMP, their Ra values of Si and C surfaces were reduced to 0.120 and 0.157 nm (Figure 4f,g), reaching the atomic-level flatness (<0.3 nm).[31] Moreover, the Si face has not any apparent scratch in AFM, showing a defect-free surface. Although the C face had a few scratches, the plowed grooves of these scratches were less than 700 pm. Furthermore, for both Si and C face, 4H-SiC could reach better surface planarization than those of the CMP processes reviewed recently by Hsieh et al[18b] and Ma et al.[30] These CMP processes included ECMP, Fenton-ECMP, ultrasonic-ECMP, PCMP, sulfate PCMP, gas-PCMP, Fenton-PCMP, and so on. These results and comparisons indicated that piezo-CMP was also a promising green advanced planarization technology for crystal SiC.

Many researchers have shown that the CMP of SiC generally underwent multi-step physical and chemical changes.[22,30] In order to understand what changes on the surface of SiC had occurred in the process of piezo-MCP, X-ray photo-electron spectra (XPS) were first used to characterize the chemical species on the surface of RS-SiC before and after polishing.

Figure 5 presents the XPS spectra of un- and polished RS-SiC surfaces by pizeo-MCP. For the surface of virgin RS-SiC (Figure 5a,b), in addition to a strong Si-C peak, two weak peaks appeared in the XPS spectra, including the Si—C—O peak in Si2p and the C—C and Si—C—O peaks in C1s. These likely originated from the natural oxidation of the functional groups of Si—C and the C—C bonds of its adhesive and sintering.[8,9b] After pizeo-MCP for 60 min (Figure 5a,b), a new weak peak was observed at 102.1 eV in Si 2p spectrum, and the binding energy much matched with that of Si—O in SiO_2. These changes in energy spectra were similar to that of RS-SiC oxidized by anodic processes reported by Yang et al.[8] It was interesting that although the two processes had similar changes of energy spectra, the polishing effect of piezo-CMP was rather different from that of the reported anodic oxidation CMP toward RS-SiC. The former could present an ultra-smooth surface of RS-SiC, as shown in Figure 3e, while the latter only offered a rough surface with oxide protrusion, as reported by Yang et al.[8] This divergence was possibly dependent on the expected selectivity of catalytic oxidation of piezo-CMP. That is, piezo-CMP possibly preferentially oxidized these protuberances of SiC surface, leading to the formation of a local softer oxide layer to be easily mechanically polished,[32] because these protuberances were subjected to greater stress than other parts from polishing pad, experienced a stronger piezocatalytic oxidation effect according to the relationship between the piezocatalytic effect and pressure as indicated in the Equation (3). Additionally, in the waste slags from piezo-CMP, a few SiC was observed from the XRD spectrum (Figure S1, Supporting Information), in addition to *t*-BT and SiO_2. SiC species were non-oxidized products while the polished workpiece itself. As a result, the appearance of these SiO_2 and SiC in the waste slags indicated that *t*-BT could act as not only a piezocatalyst but also an abrasive. It could not only selectively oxidize partly SiC to the soft oxidized layer but also mechanically remove them. The finding of the dual-role of *t*-BT was a much significant for polishing possesses because no additional oxidant, abrasive and energy was needed, which was much different from other CMPs based on advanced oxidation technology.

In order to understand the oxidation mechanism of SiC in the piezo-CMP, uminol chemiluminescence was used to

© 2023 Wiley-VCH GmbH

16136829, 2024, 21, Downloaded from https://onlinelibrary.wiley.com/doi/10.1002/smll.202310117 by Cas-Beijing Institution Of, Wiley Online Library on [28/05/2025]. See the Terms and Conditions (https://onlinelibrary.wiley.com/terms-and-conditions) on Wiley Online Library for rules of use; OA articles are governed by the applicable Creative Commons License

NANO · MICRO small
www.small-journal.com

determine the generation of oxidative ROS in various polishing processes.[33] Although it was difficult to observe the chemiluminescence of ROS due to the blocking of its polishing pad and wafer head to the piezocatalytic region, some weak blue glows in the process of oxidizing luminol were still observed in flowing slurry from the slit between the polishing pad and wafer head (Figure 5f). However, for *c*-BT abrasive, only a very faint blue glow was observed (Figure 5f), and without abrasive, no blue glow appeared (Figure 5g). It was well known that the intensity of sonochemiluminescence was directly proportional to the concentration of oxidative radicals.[33] Thus, these differences between their sonochemiluminescences showed that *t*-BT possessed a pronounced catalytic effect on the generation of the oxidative ROS, compared with *c*-BT, and no catalyst in the polishing processes.

In oxidative ROS, hydroxyl radical (•OH), superoxide radical (•O_2^-),[34] and singlet oxygen ($^1O_2$) were determined by Electron spin resonance (ESR) spectra (Figure 5), in addition to H_2O_2. As shown in Figure 5h, in the presence of *t*-BT as the abrasive, much stronger quadruple ESR peaks with the intensity ratio of 1:2:2:1 were observed. These characteristics of ESR spectra were consistent with that of typical •OH. Its peak intensity was much higher than that of •OH in the presence of *c*-BT as the abrasive. Other radicals presented similar differences to that of •OH between two abrasives (Figure 5i,j). The differences of these ROS were also consistent with the piezo-activity of the two barium titanate abrasives. This consistency denoted that these ROS did originate from the piezoelectric effect driven by frictional force in the finishing processes, and further confirmed that the polishing frictional force could be the piezoelectric effect or piezocatalytic effect.

According to the principle of common piezocatalysis, H_2O_2 could be generated, as reported by many researches.[35] Addition of Fe(II) would apparently enhance the efficiency of piezo-CMP, referring to mechanism of Fenton CMP.[35c] However, no H_2O_2 was determined in the piezo-CMP process and its MRR was only slightly increased as shown in Figure S2 (Supporting Information). Instead, a lot of bubbles-containing O_2 were generated for *t*-BT abrasive while no bubble was observed for SiO_2 abrasive, as indicated in Figure 5l,m. The generation of the bubbles-containing O_2 was possibly dependent on the H_2O_2 decomposition reactions (7) and (8), due to the thermal and chemical effects from polishing friction.[36] However, on bubble was observed when additional H_2O_2 was introduced in the polishing system using SiO_2 as an abrasive. This fact indicated that H_2O_2 decomposition of H_2O_2 was mainly via reaction (8).

$$H_2O_2 + \text{friction} \rightarrow O_2 + H_2O \quad (7)$$

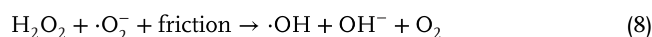

$$H_2O_2 + \cdot O_2^- + \text{friction} \rightarrow \cdot OH + OH^- + O_2 \quad (8)$$

The contributions of the three kinds of ROS to the piezo-MCP of RS-SiC were also investigated by their scavenging tests. As shown in Figure 5k, the addition of 5 mmol L^{-1} TBA (tert-butanol) as the scavenger of •OH or 5 mmol L^{-1} EDTA (ethylenediamine tetra acetic acid disodium salt) as the scavenger of hole could both significantly decrease MRR, but the latter decreased slightly more than the former. For example, EDTA could reduce 73.6% of MRR while TBA could also reduce 64.8%. Because •OH radicals came generally from the piezocatalytic oxidation of H_2O by the hole of *t*-BT,[35a,c] the small difference of this reduction after the addition of EDTA or TBA indicated that the piezo-CMP could be mainly originated from the oxidation of •OH, although the hole of *t*-$BaTiO_3$ could thermodynamically oxidize SiC. Figure 5k, still presented that NaN_3 and p-BQ (benzoquinone) could reduce MRR by 75.2% and 57.1%, respectively. Because NaN_3 was a strong reductive scavenger and could scavenge other ROS with stronger oxidation potential than that of $^1O_2$,[37] including •OH, •O_2^- and so on in the piezo-CMP, the reduction difference between •OH and NaN_3 scavenging results could be considered as the contribution of other ROS, besides •OH. In Figure 5k, only a small difference between them was observed, indicating again

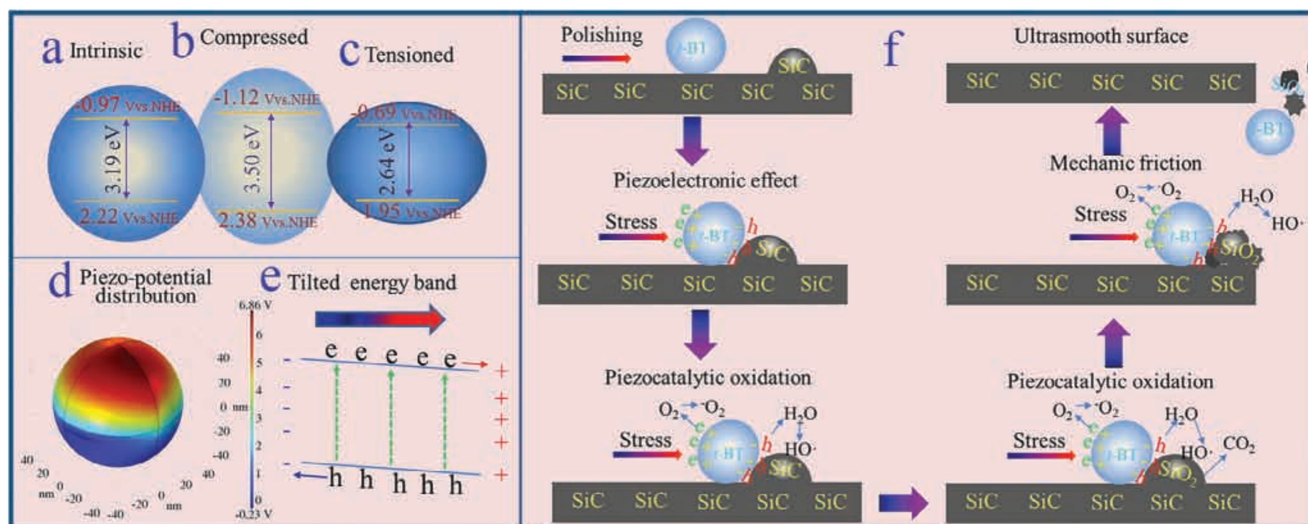

Figure 6. Mechanisms of piezo-CMP process. Left: the characteristics changes of a 45-nm *t*-BT particle with 10% friction deformation (a,b, and c: the changes of its bandgap structures calculated with DFT, d: the piezo-potential distribution simulated with COMSOL, e: tilting of energy band with piezo-potential and its effect on carrier separation). Right f): possible physical and chemical processes of piezo-CMP.

 © 2023 Wiley-VCH GmbH

16136829, 2024, 21, Downloaded from https://onlinelibrary.wiley.com/doi/10.1002/smll.202310117 by Cas-Beijing Institution Of, Wiley Online Library on [28/05/2025]. See the Terms and Conditions (https://onlinelibrary.wiley.com/terms-and-conditions) on Wiley Online Library for rules of use; OA articles are governed by the applicable Creative Commons License

that the piezo-CMP of SiC intensively depended on •OH-related reactions, not that of other ROS.

Combined with the above experimental results and refereeing to the chemical reactions of other CMP,[3,22] the mechanism of piezo-CMP could be concluded and its main polishing reactions were as follows (9–11) :

$$t - \mathrm{BT} + \text{friction stress} \rightarrow^{-e} t - \mathrm{BT}^{h+} \tag{9}$$

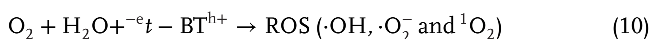

$$\mathrm{O_2} + \mathrm{H_2O} +^{-e} t - \mathrm{BT}^{h+} \rightarrow \mathrm{ROS}\ (\cdot\mathrm{OH}, \cdot\mathrm{O_2^-}\ \text{and}\ {}^1\mathrm{O_2}) \tag{10}$$

$$\mathrm{SiC} + 4 \cdot \mathrm{OH} + \mathrm{O_2} \rightarrow \mathrm{SiO_2} + \mathrm{CO_2} + 2\mathrm{H_2O} \tag{11}$$

To understand the dependence of the piezo-process on the polishing process, the change of the energy band structure of *t*-BT deformed with friction stress was calculated by density functional theory (DFT), referring to the gradient approximation method proposed by Perdew et al.[38] As shown in **Figure 6**a–c, its energy band structure was changed with stress. For example, after *t*-BT was compressed by 10%, its valence potential was raised from 2.22 V versus NHE to 2.38 V versus NHE and its conduction potential was decreased from –0.97 V versus NHE to –1.12 V versus NHE, indicating that the redox potential of the compressed *t*-BT was apparently enhanced, compared with the original *t*-BT. Simultaneously, its bandgap was increased from 3.19 to 3.50 eV. Considering that the crystal cells at the different parts of a nanoparticle were subjected to different great friction stresses, resulting in some crystal cells with various bandgaps in the stressed *t*-BT particles. According to the general theory of semiconductors, these stressed *t*-BT aggregates with various bandgaps could be regarded as composite semiconductors although they were barium titanates. Therefore, they possibly formed some dynamic homojunction in the polishing process, and their charge carrier transfer, i.e. charge carrier separation, would be improved, finally leading to the increase of above piezocatalytic reactions and CMP efficiency.

In addition to understanding the dependence of the piezo-process on the polishing process from the above changes of the bandgap structure, their relationship could further be understood from the perspective of energy band tilting or bending caused by piezoelectric fields. The piezo-potential distribution on the surface of *t*-BT particle was also calculated with COMSOL Multiphysics software. As shown in Figure 6d, for a spherical *t*-BT particle with a size of 45.4 nm, after compressed by about 10% with friction stress, its surface piezo-potentials were located in the range of (+6.86)–(–0.23) V. Although these surface piezo-potentials seem not great, their electric field intensity reached as high as about 1.6×10^6 V cm^{-1} for its particle size was much smaller. Such a great electric field intensity possibly changed many characteristics of *t*-BT, according to nanopiezotronic theory. For example, the piezoelectric field could push its thermally excited charge carriers of *t*-BT to mobile toward the opposite sides of the material and eventually lead to its energy band bending or tilting, and then drive the transportation of electrons to higher potential positions and holes to lower potential positions,[39] as shown in Figure 6e, and finally, piezoelectric field improved the efficiency of chemical polishing.

3. Conclusion

In summary, a green and effective atomically smoothing technique piezo-CMP for a third-generation semiconductor SiC was reported. Its high efficiency could be attributed to a dual effect of *t*-BT as the piezocatalyst and abrasive. That is, *t*-BT could peizocatalytically generate more active ROS in situ on the protruding sites of SiC surface to selectively oxidize them into softer SiO_2 and CO_2, and simultaneously it took the role of an abrasive to mechanically polish the softer SiO_2. In the piezo-CMP process, no additional oxidant was added, and no other energy was required apart from the original energy consumption of a common polishing device. Therefore, the piezo-CMP was a new green and effective polishing technology for SiC.

Supporting Information

Supporting Information is available from the Wiley Online Library or from the author.

Acknowledgements

T.H. and J.F. contributed equally to this work. This research was supported by the National Natural Science Foundation of China (22306034, 21976215), Natural Science Foundation of Guangdong Province (2021A1515012036), Guangzhou Municipal Science and Technology Project (202002030417) and Science and Technology Projects of Guangdong Province (2019B1515120022).

Conflict of Interest

The authors declare no conflict of interest.

Data Availability Statement

The data that support the findings of this study are available in the supplementary material of this article.

Keywords

$BaTiO_3$, piezocatalytic-CMP, polishing, SiC

Received: November 13, 2023
Revised: December 4, 2023
Published online: December 28, 2023

[1] a) A.-C. Liu, Y.-Y. Lai, H.-C. Chen, A.-P. Chiu, H.-C. Kuo, *Micromachines* **2023**, *14*, 764; b) H. Kong, J. Ibbetson, J. Edmond, *Phys. Status. Solidi.* **2014**, *11*, 621.
[2] R. T. Yadlapalli, A. Kotapati, R. Kandipati, S. R. Balusu, C. S. Koritala, *Int. J. Energy Res.* **2021**, *45*, 12638.
[3] W. Wang, X. Lu, X. Wu, Y. Zhang, R. Wang, D. Yang, X. Pi, *Adv. Mater. Interfaces* **2023**, *10*, 202202369.
[4] a) Y. Chen, P. Yu, Y. Zhong, S. Dong, M. Hou, H. Liu, X. Chen, J. Gao, C.-P. Wong, *ECS J. Solid State Sci. Technol.* **2023**, *12*, 045004; b) K. Hamada, M. Nagao, M. Ajioka, F. Kawai, *IEEE Trans. Electron Devices* **2015**, *62*, 278.

© 2023 Wiley-VCH GmbH

16136829, 2024, 21, Downloaded from https://onlinelibrary.wiley.com/doi/10.1002/smll.202310117 by Cas-Beijing Institution Of, Wiley Online Library on [28/05/2025]. See the Terms and Conditions (https://onlinelibrary.wiley.com/terms-and-conditions) on Wiley Online Library for rules of use; OA articles are governed by the applicable Creative Commons License

[5] A. Isohashi, P. V. Bui, D. Toh, S. Matsuyama, Y. Sano, K. Inagaki, Y. Morikawa, K. Yamauchi, *Appl. Phys. Lett.* **2017**, *110*, 20.
[6] J. Seo, *J. Mater. Res.* **2021**, *36*, 235.
[7] a) Z. Yuan, Y. He, X. Sun, Q. Wen, *Wafer. Mater. Manuf. Processes* **2018**, *33*, 1214; b) H. Aida, T. Doi, H. Takeda, H. Katakura, S.-W. Kim, K. Koyama, T. Yamazaki, M. Uneda, *Curr. Appl. Phys.* **2012**, *12*, S41; c) B. Meng, D. Yuan, J. Zheng, P. Qiu, S. Xu, *Appl. Surf. Sci.* **2020**, *500*, 144039.
[8] X. Yang, X. Yang, H. Gu, K. Kawai, K. Arima, K. Yamamura, *J. Electrochem. Soc.* **2022**, *169*, 023501.
[9] a) H. Lee, H. Kim, H. Jeong, *Int. J. Precis. Eng. Man-GT.* **2022**, *9*, 349; b) Y. He, Z. Yuan, S. Song, X. Gao, W. Deng, *Int. J. Precis. Eng. Manuf.* **2021**, *22*, 951.
[10] a) X. Y. Kong, Z. L. Wang, *Nano Lett.* **2003**, *3*, 1625; b) Y. Jia, K. Zhang, *Nano Energy* **2022**, *96*, 107103.
[11] a) X. Wang, J. Song, J. Liu, Z. L. Wang, *Science* **2007**, *316*, 102; b) Y. Qin, X. Wang, Z. L. Wang, *Nature* **2008**, *451*, 809.
[12] a) M. B. Starr, J. Shi, X. Wang, *Angew. Chem., Int. Ed.* **2012**, *51*, 5962; b) M. Wang, B. Wang, F. Huang, Z. Lin, *Angew. Chem., Int. Ed.* **2019**, *58*, 7526; c) S. Lan, J. Feng, Y. Xiong, S. Tian, S. Liu, L. Kong, *Environ. Sci. Technol.* **2017**, *51*, 6560; d) Z. Chen, H. Zhou, F. Kong, M. Wang, *Appl. Catal. B* **2022**, *309*, 121281.
[13] Y. Wang, X. Wen, Y. Jia, M. Huang, F. Wang, X. Zhang, Y. Bai, G. Yuan, Y. Wang, *Nat. Commun.* **2020**, *11*, 1328.
[14] J. Feng, Y. Fu, X. Liu, S. Tian, S. Lan, Y. Xiong, *ACS Sustainable Chem. Eng.* **2018**, *6*, 6032.
[15] J. Feng, T. Zhang, J. Sun, J. Zhu, W. Yan, S. Tian, Y. Xiong, Y. Xiong, *Water Res.* **2022**, *209*, 117922.
[16] P. Zhu, Y. Chen, J. Shi, *Adv. Mater.* **2020**, *32*, 2001976.
[17] a) F. Bößl, T. P. Comyn, P. I. Cowin, F. R. García-García, I. Tudela, *Chem. Eng. J. Adv.* **2021**, *7*, 100133; b) S. Lan, C. Yu, E. Wu, M. Zhu, D. Dionysiou, *ACS ES&T Eng.* **2022**, *2*, 101.
[18] a) Y. Zhou, G. Pan, X. Shi, L. Xu, C. Zou, H. Gong, G. Luo, *Appl. Surf. Sci.* **2014**, *316*, 643; b) C. Hsieh, C. Chang, Y. Hsiao, C. Chen, C. Tu, H. Kuo, *Micromachines* **2022**, *13*, 1752.
[19] X. Shen, Q. Tu, H. Deng, G. Jiang, X. He, B. Liu, K. Yamamura, *Appl. Phys. A* **2016**, *122*, https://doi.org/10.1007/s00339-016-9896-y.
[20] a) F.-S. Yen, H.-I. Hsiang, Y.-H. Chang, *Jpn. J. Appl. Phys* **1995**, *34*, 6149; b) X. Li, W.-H. Shih, *J. Am. Ceram. Soc.* **1997**, *80*, 2844.
[21] a) M. Mahrova, M. Conte, E. Roman, R. Nevshupa, *J. Phys. Chem. C* **2014**, *118*, 22544; b) B. Stefanovic, K. F. Pirker, T. Rosenau, A. Potthast, *Carbohydr. Polym.* **2014**, *111*, 688; c) M. Wu, Y. Xu, Q. He, P. Sun, X. Weng, X. Dong, *J. Colloid Interface Sci.* **2022**, *622*, 602.
[22] G. Pan, Y. Zhou, G. Luo, X. Shi, C. Zou, H. Gong, *J. Mate. Sci.-Mater. Electron.* **2013**, *24*, 5040.
[23] B. D. Begg, E. R. Vance, J. Nowotny, *J. Am. Ceram. Soc.* **1994**, *77*, 3186.
[24] J. Yao, J. Li, H. Liu, Z. Wang, Y. Zhu, J. Su, *Int. J. Mod. Phys B* **2022**, *36*, 2240027.
[25] Q. Zhang, J. Pan, X. Zhang, J. Lu, Q. Yan, *Wear* **2021**, *203649*, 472.
[26] a) J. M. Wu, W. E. Chang, Y. T. Chang, C.-K. Chang, *Adv. Mater.* **2016**, *28*, 3718; b) Y. Feng, L. Ling, Y. Wang, Z. Xu, F. Cao, H. Li, Z. Bian, *Nano Energy* **2017**, *40*, 481.
[27] a) Y. Gao, S. Li, B. Zhao, Q. Zhai, A. Lita, N. S. Dalal, H. W. Kroto, S. F. A. Acquah, *Carbon* **2014**, *77*, 705; b) W. Qian, W. Yang, Y. Zhang, C. R. Bowen, Y. Yang, *Nano-Micro Lett.* **2020**, *12*, 149.
[28] a) X. Shen, Y. Dai, H. Deng, C. Guan, K. Yamamura, *Opt. Express* **2013**, *21*, 14780; b) J. Yan, Z. Zhang, T. Kuriyagawa, *Int. J. Mach. Tool. Manu.* **2009**, *49*, 366.
[29] X. Shen, Q. Tu, H. Deng, G. Jiang, K. Yamamura, *Opt. Eng.* **2015**, *54*, 055106.
[30] G. Ma, S. Li, F. Liu, C. Zhang, Z. Jia, X. Yin, *Crystals* **2022**, *12*, 101.
[31] J. Deng, J. Lu, S. Zeng, Q. Xiong, Q. Yan, J. Pan, *Surf. Interfaces.* **2022**, *29*, 101646.
[32] X. Yang, R. Sun, Y. Ohkubo, K. Kawai, K. Arima, K. Endo, K. Yamamura, *Electrochim. Acta* **2018**, *271*, 666.
[33] C. Kong, Y. Yoon, Y.-D. Choi, S.-J. Lee, J. Oh, J. Han, N. Her, *J. Nanoelectron. Optoelectron.* **2012**, *7*, 522.
[34] a) D. Ma, W. Liu, Y. Huang, D. Xia, Q. Lian, C. He, *Environ. Sci. Technol.* **2022**, *56*, 3678; b) S. Zhan, H. Huang, C. He, Y. Xiong, P. Li, S. Tian, *Appl. Catal. B* **2023**, *321*, 122040.
[35] a) C. Hu, J. Hu, Z. Zhu, Y. Lu, S. Chu, T. Ma, Y. Zhang, H. Huang, *Angew. Chem., Int. Ed.* **2022**, *61*, 202212397; b) L. Fang, K. Wang, C. Han, X. Li, P. Li, J. Qiu, S. Liu, *Chem. Eng. J.* **2023**, *461*, 141866; c) W. Lv, L. Kong, S. Lan, J. Feng, Y. Xiong, S. Tian, *J. Chem. Technol. Biotechnol.* **2017**, *92*, 152.
[36] a) J. Deng, Q. Zhang, J. Lu, Q. Yan, J. Pan, R. Chen, *Precis. Eng.* **2021**, *72*, 102; b) Y. Yu, X. Liu, H. Duan, J. Yang, Z. Qiao, J. Li, J. Li, *Mater. Lett.* **2020**, *276*, 128025.
[37] K. Wang, C. Han, J. Li, J. Qiu, J. Sunarso, S. Liu, *Angew. Chem., Int. Ed.* **2022**, *61*, 202110429.
[38] a) J. P. Perdew, K. Burke, M. Ernzerhof, *Phys. Rev. Lett.* **1996**, *77*, 3865; b) J. Heyd, G. E. Scuseria, M. Ernzerhof, *J. Chem. Phys.* **2003**, *118*, 8207; c) J. Liu, *J. Phys. Chem. C* **2015**, *119*, 28417.
[39] O. Sudhir Ekande, M. Kumar, *Chem. Eng. J.* **2023**, *458*, 141454.

© 2023 Wiley-VCH GmbH

16136829, 2024, 21, Downloaded from https://onlinelibrary.wiley.com/doi/10.1002/smll.202310117 by Cas-Beijing Institution Of, Wiley Online Library on [28/05/2025]. See the Terms and Conditions (https://onlinelibrary.wiley.com/terms-and-conditions) on Wiley Online Library for rules of use; OA articles are governed by the applicable Creative Commons License